Testing of Damaged Single-Bay Reinforced Concrete Frames Strengthened with Masonry Infill Walls

Grubišić, Marin; Kalman Šipoš, Tanja; Grubišić, Ante; Pervan, Benjamin

GRAĐEVINSKI I ARHITEKTONSKI FAKULTET OSIJEK
Faculty of Civil Engineering and Architecture Osijek

SVEUČILIŠTE JOSIPA JURJA STROSSMAYERA U OSIJEKU

dabar
DIGITALNI AKADEMSKI ARHIVI I REPOZITORIJI

Article

Testing of Damaged Single-Bay Reinforced Concrete Frames Strengthened with Masonry Infill Walls

Marin Grubišić [1,*], Tanja Kalman Šipoš [1], Ante Grubišić [2] and Benjamin Pervan [3,†]

1   Faculty of Civil Engineering and Architecture, University of Osijek, 3 Vladimir Prelog Street, HR-31000 Osijek, Croatia; tkalman@gfos.hr
2   TRINAS Project Ltd., 14 Dubrovačka Street, HR-31000 Osijek, Croatia; ante.grubisic@trinas.hr
3   Institute IGH PLC, 1 Janka Rakuše Street, HR-10000 Zagreb, Croatia; benjaminpervan@gmail.com
*   Correspondence: marin.grubisic@gfos.hr; Tel.: +385-95-823-15-75
†   Current address: Dalekovod PLC, 4 Marijana Čavića Street, HR-10000 Zagreb, Croatia.

Abstract: Despite achieving consensus and having current knowledge on the behaviour and contribution of masonry infill walls, there remain unresolved issues regarding their nonlinear behaviour as a method for strengthening existing reinforced concrete (RC) frames with effective modifications, primarily infills and the interconnection of infills and frames. The challenge for safely and economically designing frames with competent walls is to utilise the stiffening benefits while ensuring that the increased lateral forces and reduced drift capacity do not hinder performance. This study aims to investigate the potential of using masonry infill to strengthen previously slightly damaged RC frames. Experimental tests were conducted on previously slightly damaged RC frame specimens infilled with vertically hollowed-clay and solid-clay masonry units, connected to the frame elements using traditional methods (i.e., avoiding the use of modern composite materials). These strengthened infilled frame structures were subjected to constant vertical and cyclic lateral loading, which revealed improved stiffness, strength, and damping characteristics, enhancing their overall behaviour. As the main novelties, the study found that when damaged RC frames were strengthened with masonry infill walls, their performance resembled that of undamaged infilled RC frames. The strengthened infilled frame structures exhibited enhanced stiffness, strength, and hysteretic damping. The increase in stiffness was observed regardless of the type of masonry units and the strengthening technique employed. However, the improvements in strength and hysteretic damping were influenced by the specific masonry units, particularly their robustness, and the chosen reinforcement method.

Keywords: reinforced-concrete frame; masonry infill; seismic strengthening; strengthened infilled frames; experimental testing

1. Introduction

The use of masonry walls to infill RC frames is prevalent in Southern and Eastern Europe and the contribution of these infills is well understood by researchers and engineers. However, accurately considering the complex interaction between the infill and the frame during design is challenging given that it is a highly nonlinear problem. As a result, the contribution of infills is frequently overlooked not only during the design phase but also in the seismic evaluation and strengthening of existing or damaged buildings.

The research community has extensively studied masonry infills due to their significant contribution to a structure's lateral strength and stiffness. In many cases, this contribution is beneficial, as they act as a weaker version of shear walls. However, uneven height-wise or floor-wise positioning or partial construction within a bay's height can lead to adverse effects [1,2]. Considering the positive effects of infills and their low construction cost, the authors have proposed using them as strengthening elements. As a potential seismic strengthening technique, the primary objective and novelty of this research are to

investigate the positive effects of adding different types of traditional reinforced masonry infills connected to existing RC frame elements for seismic actions.

A preliminary assessment of the seismic capacity of existing (and damaged) RC buildings is essential to the planning, design, and selection of an appropriate seismic strategy for the strengthening of buildings. This assessment often involves nonlinear numerical investigations using simplified displacement-based procedures to derive capacity curves that can provide a quick and reliable estimate of the building's seismic performance. The numerical results obtained from the simplified displacement-based procedures should typically be validated and supplemented with the results of nonlinear dynamic analyses [3].

1.1. A Concise Overview of Masonry Infill Behaviour

The use of masonry infill walls can have both positive and negative effects, as reported in previous studies [4]. The presence of an infill wall alters the lateral-load response mechanisms of the composite structure, and the behaviour of the structure is not simply the sum of its components [5–8]. Strengthened infilled frame structures have been found to exhibit higher stiffness, strength, and hysteretic energy-dissipation capacity than bare-frame structures, as noted in previous studies [9–12,12–15]. However, they also experience higher seismic forces and may have some detrimental global effects, such as the formation of a soft storey mechanism, increased torsional effects, and pronounced local effects, such as shear failure of columns, beams, and beam-column joints.

When subjected to lateral loading, strengthened infilled frame structures behave as composite structures, similar to those experienced during an earthquake. Failure typically initiates in the weaker component, whether it be the RC frame or masonry infill, and can manifest in various modes. Therefore, experimental research plays a crucial role in accurately assessing the behaviour of such structures. This is particularly relevant when considering the use of masonry infill as a strengthening technique for existing or damaged RC frames, as it is necessary to determine the impact of various masonry-strengthening methods on the lateral load-carrying capacity of the RC frames [16–20].

Previous experimental investigations on the behaviour of RC frames with masonry infill walls under static and dynamic lateral cyclic loads have been conducted [21–32]. The findings have demonstrated that infill walls can significantly increase the strength and stiffness of RC frames compared to bare frames. While conventional seismic design mainly focuses on acceleration and strength, it can be challenging to recognise the benefits of increased stiffness. However, both research and field evidence [6,33–41] have indicated that increased stiffness is advantageous as it reduces the magnitude of the deformations caused by ground motions. This study revealed that the increase in lateral forces and reduction in drift capacity did not impede the anticipated performance of buildings during earthquakes.

The addition of masonry infill walls to RC frames can enhance the seismic performance of a building and increase its overall seismic performance level. This is an economical solution for strengthening relatively weak or damaged RC frames. To investigate this, six 1:2.5 scaled one-storey one-bay damaged "strong" RC frames (designed according to Eurocode 8) were strengthened with two types of masonry infill walls (solid-clay brick and vertically hollowed-clay block units with mortar) in three different ways to secure the shear connection between the infill and the frame. The specimens were subjected to constant vertical and cyclic lateral loading, and their test results were compared with those of undamaged bare frames and undamaged RC frames with hollow-clay masonry infill. The results showed that the addition of masonry infill increased the initial stiffness, maximum lateral strength, and hysteretic damping, and decreased the drift demand. The behaviour of damaged and undamaged RC frames with masonry infill was similar, and the strength of the masonry units was the most important parameter for the behaviour of the strengthened infilled frames. The behaviour factor of the strengthened infilled frames was between that of confined masonry and RC frame structures. All strengthened infilled frames had drift capacities greater than 1.2%, and their expected average nonlinear drifts when exposed to earthquake ground motions in the highest seismic regions of Croatia

remained below that value [10]. The highest seismic regions refer to country areas with the highest seismic hazard risk in Croatia, where the maximum expected acceleration is 0.36 g for a return period of 475 years and soil type A, as indicated by the earthquake hazard maps for Croatia in the national annex to Eurocode 8 [42]. Furthermore, following the strong earthquakes in Zagreb and Petrinja in 2020, which caused significant destruction and losses, the Croatian public's awareness of the earthquake hazard in Croatia has increased significantly over the last three years [43].

1.2. Overview of Seismic Retrofitting for Existing RC Structures

Improving the seismic resistance of existing RC structures is crucial for ensuring their safety and functionality during earthquakes. There are several widely adopted strengthening or retrofitting techniques that can be used to enhance the seismic performance of these structures.

On the basis of how they "treat" the structure, seismic upgrading techniques can be divided into two broad categories. First, there are those that operate at the element level (*Local* measures), followed by those that operate on the entire structure (*Global* measures). Obviously, when it comes to enhancing a specific structure, it may be necessary to combine various techniques, taking into account its unique characteristics, in order to provide a cost-effective strengthening scheme. On the basis of their age and the materials used, the seismic intervention techniques can also be subdivided into conventional and novel techniques.

The *local* upgrading techniques involve the application of measures to particular structural elements of a building in order to improve their mechanical properties. The general concept is to add some type of external reinforcement to the existing beam/column/joint member in order to increase its flexural and/or shear capacity and ductility [1–3,44–46]. Local strengthening measures can be classified into the following categories:

1. *RC Jacketing*: This method involves adding a layer of new concrete around the existing structural members. Reinforcement bars are typically used to connect the new concrete layer to the existing structure, which can result in increased strength, stiffness, and confinement of the RC members.
2. *Steel Jacketing*: Steel plates or jackets are attached to the existing RC columns or beams to increase their strength and stiffness. This technique enhances the load-carrying capacity of the structural members, preventing buckling or premature failure during earthquakes.
3. *Fibre Reinforced Polymer (FRP) Wrapping*: FRP materials, such as carbon, glass, or aramid fibres, can be applied as sheets or laminates to the surface of the RC structure. This technique increases the confinement of concrete, resulting in improved strength, ductility, and energy dissipation capacity during seismic events.
4. *Textile Reinforced Mortar* (*TRM*): TRM has demonstrated superior performance to FRP as a strengthening material at high temperatures, whereas the TRM mechanical behaviour has also been found satisfactory after exposure to fire. These textiles are meshes of long woven, knitted, or even unwoven fibre rovings in at least two (usually orthogonal) orientations.
5. *Hybrid Jacketing Systems*: FRP/TRM jackets with near surface mounted (NSM) reinforcement, FRP and steel jacketing, Steel/FRP and high-performance materials.

When a significant increase in lateral load capacity or stiffness is required for a structure, local retrofitting measures may not be sufficient or may result in uneconomical solutions. In these cases, *global* measures are utilised, focusing on either increasing the structure's lateral strength and stiffness or reducing seismic demand. Increasing lateral strength and stiffness is typically accomplished by adding new structural elements to the existing building, which significantly enhances its lateral resistance. Alternatively, reducing earthquake-induced forces on a structure can be achieved through the use of base isolation systems or energy-dissipating devices, such as dampers. This overview presents state-of-the-art retrofitting approaches suitable for RC buildings [1–3,44–46]. Global strengthening measures can be classified into the following categories:

1. *Bracing Systems*: These new elements help manage lateral loads while working alongside existing frame members, requiring careful attention to their connections and the increased axial loads on columns. Retrofitting work typically occurs on the structure's outer frames, minimising living space reduction and occupancy disruption. Various bracing types, such as concentric bracing, can be employed in RC structures to resist horizontal seismic forces through axially loaded members. These systems include concentric braces, eccentric braces, buckling-restrained braces (BRBs), and steel exoskeletons.

2. *External Post-Tensioning*: This technique involves applying prestressing force to the existing structure using high-strength steel tendons. These tendons are anchored to the structure and apply a compressive force, which can improve the overall structural integrity and capacity to resist seismic loads.

3. *Structural RC Walls*: Adding structural RC walls or moment-resisting frames (MRF) can enhance the lateral load resistance and overall stability of the structure. RC shear walls are highly effective at minimising inter-story drifts, mitigating irregularities, and averting soft-story failure mechanisms. These elements help redistribute seismic forces, reducing the demand on the existing structural members. This includes precast concrete panels (PCP) as an alternative way of strengthening RC frames via infilling.

4. *Infill Walls*: Masonry or RC infill walls can be added between the structural frames of a building to increase its stiffness and lateral load resistance. These walls can also provide additional energy dissipation capacity during seismic events. This includes: addition/modification of infills, unreinforced and lightly reinforced masonry infills, engineered cementitious composites (ECC)-strengthened masonry infills, FRP-strengthened masonry infills, TRM-strengthened masonry infills, TRM-jacketing combined with thermal insulation for integrated retrofitting, and isolated masonry infills.

5. *Rocking walls*: Shear walls can be designed to allow uplifting and rocking at their base, resulting in minimal damage, no loss of strength or stiffness, and no residual deformations, aided by the use of tendons. Energy dissipation is achieved through the rocking action, and it can be enhanced by incorporating additional dissipating devices. Reinforcement is necessary for the corner regions of the wall due to the high compressive strains induced by the rocking action, and shear keys must be installed at the wall's end to prevent sliding.

6. *Base Isolation*: This technique separates the structure from the ground using isolation bearings or devices, which allow the structure to move independently from the ground motion during an earthquake. This significantly reduces the seismic forces transmitted to the structure, minimising the potential for damage.

7. *Passive Energy Dissipation Systems*: The installation of passive energy dissipation systems is an alternative to base isolation in terms of reducing the seismic demands of a given building. The purpose of these devices is to dissipate the greatest amount of seismic energy so that the remaining structural components are not damaged. Visco-elastic dampers, friction dampers, viscous-fluid dampers, tuned mass dampers (TMDs), and tuned liquid dampers (TLDs).

2. Damaged RC Frame Specimens

This study aimed to investigate whether the use of masonry infill walls could enhance the resilience of RC frames or repair those that have been slightly damaged. To test this hypothesis, an experimental program was created. The objective was to develop a composite structure of frame and infill wall that could withstand displacement cycles in the nonlinear range by improving the displacement capacity.

As part of a larger research project [47], ten RC frames were constructed and tested under constant vertical and in-plane reversed cyclic loading. The RC frame specimens were designed in accordance with EC2 [48] and EC8 [49,50] standards, without considering the influence of masonry infill, as DCM-ductility-class structures. The specimens had dimensions of 2.2 m width and 1.5 m height, with columns and beam cross-sections of

20×20 cm and 12×20 cm, respectively. The span-to-height ratio of the opening was $h/l = 0.72$. The concrete materials used were C30/37, and the reinforcement was B500B. The longitudinal reinforcement ratio of the columns was $\rho_v = 2.36\%$, while the beams had reinforcement ratios of $\rho_v = 1.31\%$ at the mid-span and $\rho_v = 3.27\%$ at the ends. Figure 1 provides details of the specimens, cross-sections, and reinforcement. All frames underwent previous testing twice, where they were pushed to drifts of about 1.5% [9,51]. Furthermore, drift will be referred to as IDR, i.e., inter-storey drift ratio, expressed as rotation, i.e., storey displacement divided by storey height, in percentages.
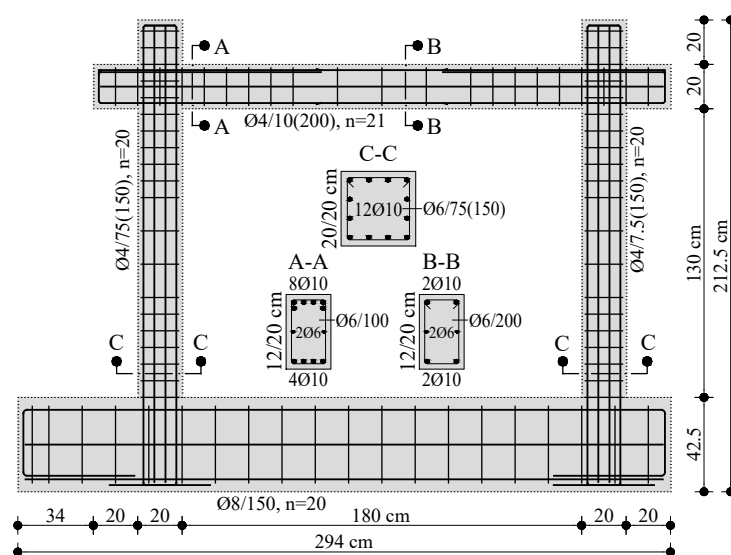

Figure 1. RC frame specimens, reinforcement details, and element cross-sections (A-A, B-B and C-C).

The observed damage on the specimens ranged from *Moderate* to *Heavy*, with *Cracks* to *Large cracks* (terminology defined in [52]) in columns and beam-column joints, spalling of concrete cover, buckling of reinforcing bars, and concrete crushing. To repair such damage, spalled and loose concrete was replaced with fast-setting concrete mortar, and masonry infill walls were connected to the frame in three traditional ways. Two types of masonry units with different strength properties were used: high-strength solid-clay bricks and medium-strength hollow-clay block units. The mechanical properties of the concrete, steel, masonry units, mortar, and masonry wallets were tested according to relevant codes and were combined as part of wider experimental tests of related systems as part of a joint scientific project [9,51,53,54] and summarised in Table 1 in terms of mean values and coefficients of variation (COV).

Table 1. Mean values and coefficients of variation (COV) of mechanical properties (masonry, steel reinforcement, and concrete).

	Masonry Infill with Cement-Lime Mortar		Frame Structure Materials			
	Hollow-Clay Block	Solid-Clay Brick	Steel Reinforcement, B500B		Concrete, C30/37	
E_m	8100 MPa (0.20)	1700 MPa (0.18)	E_s	196 GPa (0.06)	E_c	34.90 GPa (0.04)
f_m	4.60 MPa (0.12)	5.20 MPa (0.10)	f_{sym}	545 MPa (0.08)	f_{cm}	45.00 MPa (0.15)
f_{mt}	0.16 MPa (0.14)	0.20 MPa (0.10)	f_{su}	645 MPa (0.10)	f_{ctm}	3.60 MPa (0.10)
ν_m	0.10 (0.21)	0.15 (0.19)	k_s	0.05 (0.06)	ν_c	0.20 (0.20)

E_m is mean modulus of elasticity of masonry, f_m is mean compressive strength of masonry, f_{mt} is mean tensile strength of masonry, ν_m is Poisson's ratio of masonry, E_s is mean modulus of elasticity of steel, f_{sym} is mean yield strength of steel, f_{su} is mean ultimate tensile strength of steel, k_s is hardening coefficient of steel, E_c is mean modulus of elasticity of concrete, f_{cm} is mean compressive strength of concrete, f_{ctm} is mean tensile strength of concrete, ν_c is Poisson's ratio of concrete. In parentheses are coeff. of variation.

3. Strengthening of Damaged RC Frames with Masonry Infill Wall

The addition of masonry infill can be an effective way to strengthen an existing or damaged RC frame structure and improve its ability to withstand moderate earthquakes. There are several traditional and innovative methods for introducing masonry infill that can increase the stiffness, strength, and damping characteristics of the structure [16–20]. However, there is currently a lack of knowledge about how the infill behaves and reliable methods for evaluating the new structural capacity in relation to the seismic demands it may face.

There are new and innovative ways to strengthen RC frames against earthquakes, such as using fibre composites, energy-dissipation devices, and seismic isolation techniques. However, in this study, we focused on more traditional methods, which are less expensive and easier to implement. An experimental study was conducted to investigate several ways of strengthening RC frames with masonry infill walls, as shown in Figure 2.
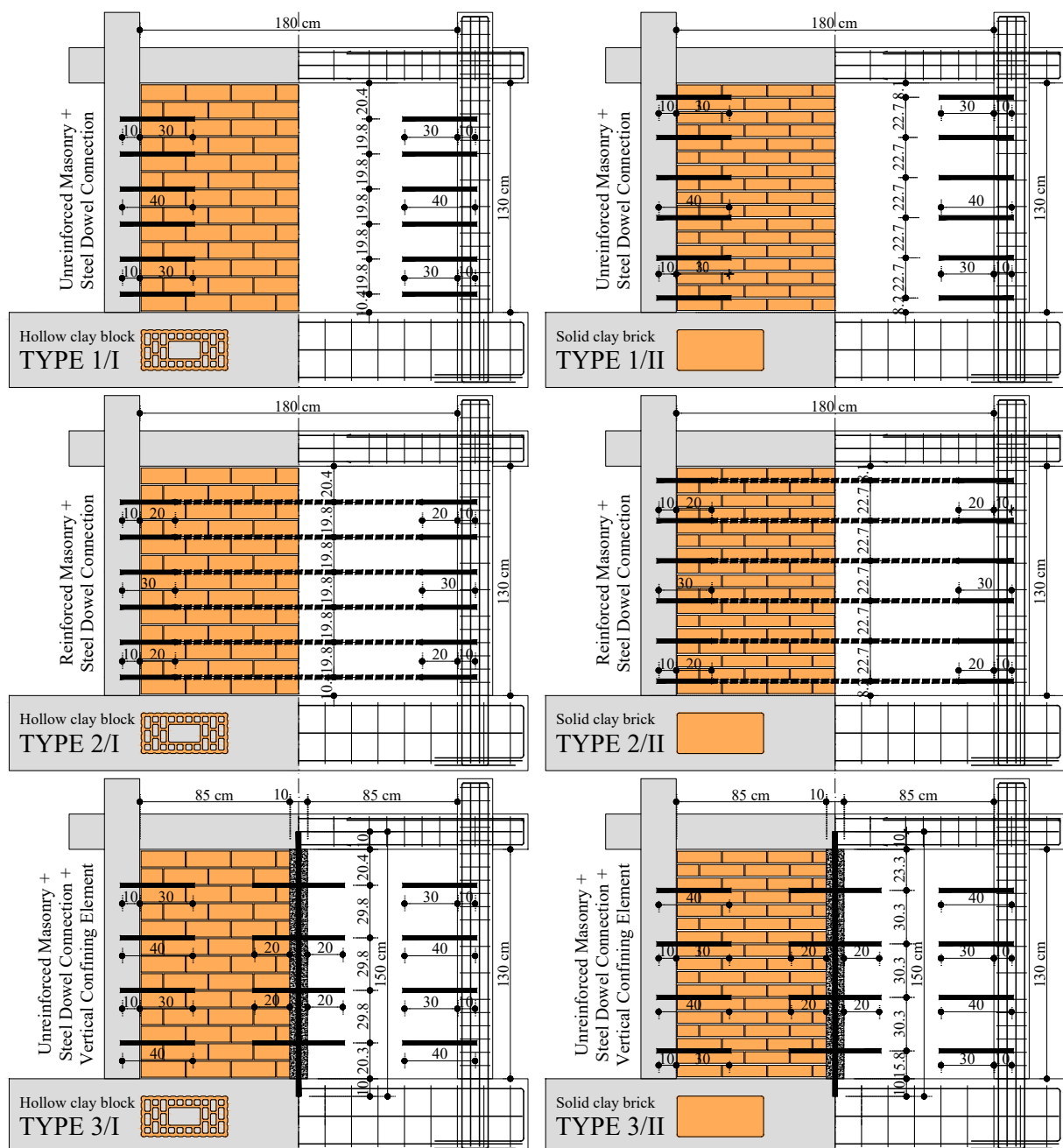

Figure 2. The applied methods of the masonry infill walls. Strengthening methods are shown with and without reinforcement details, i.e., the specimens do not contain any openings.

(A)　Unreinforced masonry wall connected to the surrounding RC frame by steel dowels (*TYPE 1/I—hollow-clay units, TYPE 1/II—solid-clay units*);

(B)　Reinforced masonry wall connected to the surrounding RC frame by steel dowels (*TYPE 2/I—hollow-clay units, TYPE 2/II—solid-clay units*);

(C)　Unreinforced masonry wall strengthened with additional vertical tie-columns and connected to these and the surrounding frame by steel dowels (*TYPE 3/I—hollow-clay units, TYPE 3/II—solid-clay units*).

Figure 2 illustrates various strengthening methods for RC frames using masonry infill walls. The left side of each image shows a front view of the specimen, while the right side depicts a schematic representation of the frame strengthening method. The tie-column contains two ribbed rebars with a diameter of 6 mm, mounted in parallel and spaced 8 cm apart in a 12 cm thick infill wall (all infill walls are 12 cm thick). The rebars are anchored to the foundation beam and upper beam with a 10 cm length, using cementitious anchoring grout, a specialised commercial product for anchoring structural steelwork. The same anchoring technique was used for the reinforced infill and frame columns. The specimens used in the study did not have any openings and were previously slightly damaged RC frames that had undergone light repairs by replacing the spalled concrete. The masonry infill walls were produced in situ using cement-lime mortar with a nominal strength of 5 MPa and a volume proportion of *cement:lime:sand* = 1:1:5. The thickness of the horizontal bed joints was 1 cm, and the vertical joints were completely filled. The tests were conducted after the masonry wall had aged for 28 days. Two specimens were tested earlier and were used as reference values for the study.

(D)　Bare reinforced-concrete frame (*TYPE 0/REF*);

(E)　Unreinforced masonry wall with hollow-clay masonry units without any shear connection to the surrounding RC frame (except adhesion *TYPE 1/REF*). The RC frame was undamaged prior to testing.

4. Testing of the Strengthened Specimens

The specimens were tested at the University of Osijek, Croatia, within a rigid steel test frame that was anchored to a strong floor and supported by inclined braces, as shown in Figure 3. In the experiment, cyclic lateral loading was applied to the beams' ends, while constant vertical loading was applied to the columns' tops using hydraulic actuators. Throughout the test, various data were continuously recorded, including the applied loads at each of the four loading points, the vertical and horizontal displacements of the specimen at the beam/column ends, the control displacements of the foundation beam, the elongations of diagonals on the frame, and the local strains at the frame's critical points (column- and beam-ends) using linear transducers as strain gauges. In addition, displacement transducers were placed on a separate scaffolding to measure global deformations accurately. All data were collected and recorded at 25 Hz using Dewetron data-acquisition devices and the software DeweSoft 7.

The experiments applied a constant vertical load of 365 kN to each column, which corresponds to the target axial load ratio of 0.20, which is determined based on the critical frame according to Eurocode 8 (DCM) of the designed hypothetical RC building [10,55], and was kept as constant as possible using hydraulic valves. The experiment began as force-controlled, and when stiffness decreased, it became displacement-controlled. Initially, the cyclic quasi-static lateral load was applied in increments of 10 kN, but later, horizontal displacements were increased in increments of 1.0 mm. To prevent one-sided progressive failure, two loading cycles were performed for each loading phase. When the infill panel experienced significant degradation associated with one-sided progressive failure, lateral loading was applied from one side only (pushover) up to the maximum drift allowed by the testing setup. The testing setup allowed for an average of 60 cycles for all tests. Figure 4 shows a detailed illustration of the loading process. During each loading stage, the specimens were visually inspected and photographed. The initial and significant cracks were identified and marked, as shown in Figure 5. Other significant phenomena that

occurred during the testing, such as masonry crushing, crack developments in masonry and concrete, and crack patterns, were also documented.
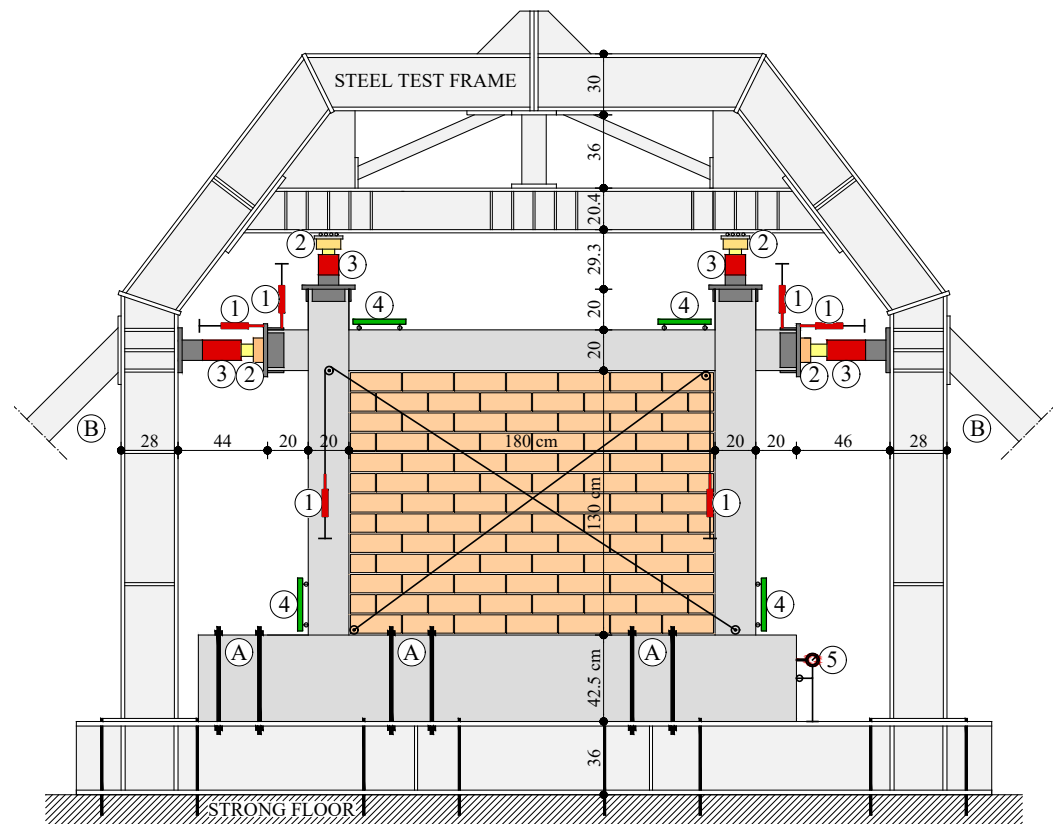

Figure 3. Test setup with loading and measuring instruments (where (A) bolts, (B) inclined steel braces, (1) LVDTs, (2) force transducers, (3) hydraulic actuators, (4) deformeters (extensometers) and (5) dial gauge). Vertical actuators contain rollers supported by a steel beam, to ensure horizontal sliding boundary condition.
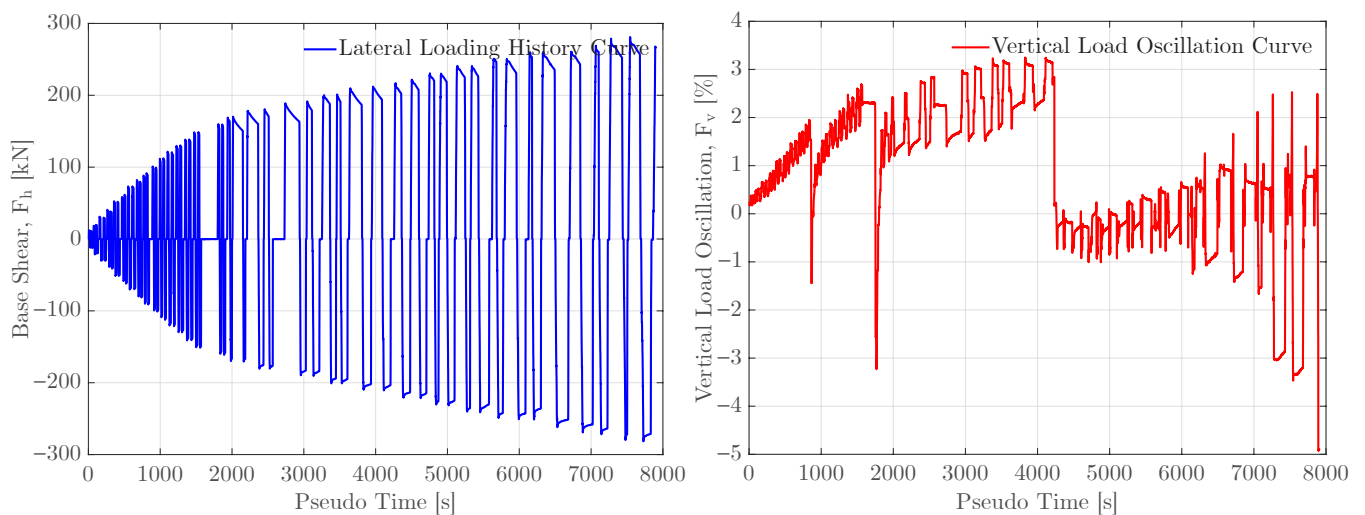

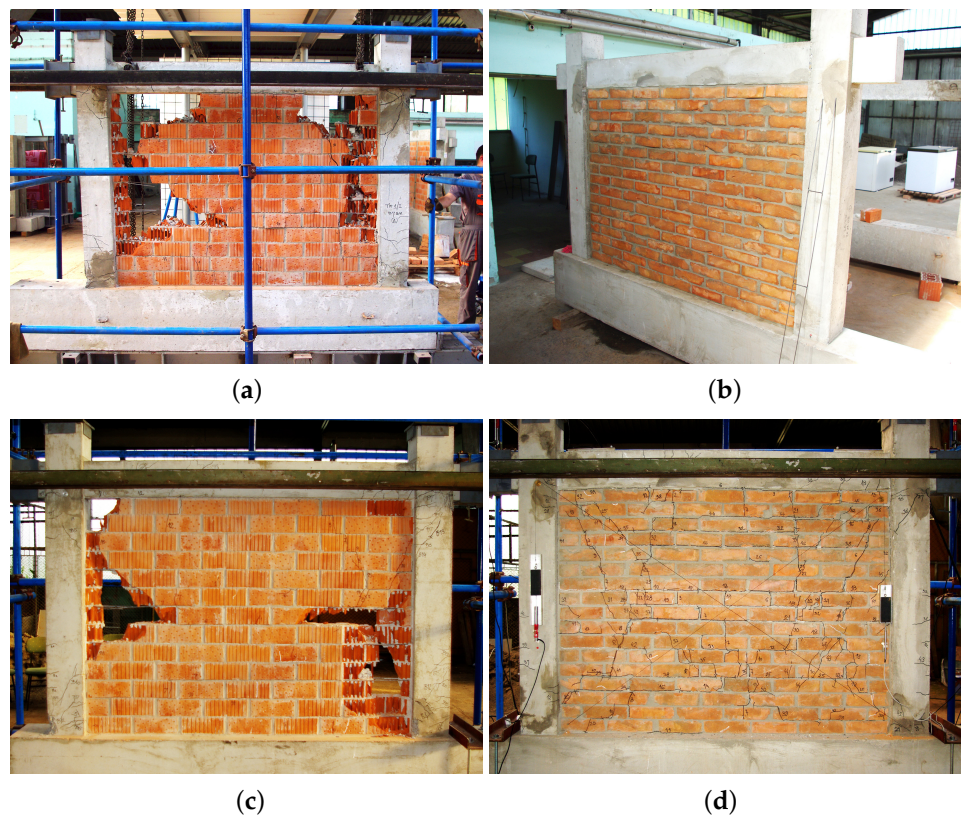**Figure 4.** Time-history of the applied lateral cyclic (**left**) and vertical load (**right**).

Figure 5. Photographs of the specimens during various phases: (**a**) specimen TYPE 1/I at 1.14% IDR (end of the experiment); (**b**) specimen TYPE 1/II before the experiment; (**c**) specimen TYPE 2/I at 1.50% IDR (the end of the experiment); and (**d**) the specimen TYPE 1/II at 1.18% IDR (the end of the experiment).

5. Test Results

The RC frame specimens used in the experiment had already undergone two tests and had been slightly damaged (up to the yield point). The masonry infill wall was added to retrofit the structure, and the strengthened infilled frames were then tested as described. The results of the experiment are presented in the following forms: hysteresis loops, response envelope, stiffness degradation curves, failure modes, and damage grades at different drift levels.

5.1. Failure Modes and Damage Grades

In all tests, the masonry infill was found to be the first to fail. The masonry infill failure could be classified into four distinct modes, namely *Corner Crushing* (*CC*), *Diagonal Compression* (*DC*), *Bed Joint Sliding Shear* (*SS*) and *Horizontal Sliding Shear* (*HSS*), as described in previous studies [5,56]. On the other hand, the RC frame exhibited three different failure modes, namely *Tensile cracking failure of the columns* (*TC*), *Shear cracking failure of the columns* (*SC*) and *Beam–column joint crack* (*BCC*).

The crack patterns that occurred at the maximum measured drift are presented in Figure 6. The masonry units' behaviour and the resulting crack patterns depended on the type of unit used. The first cracks were observed in hollow-clay masonry units at drift levels ranging from 0.075 to 0.12%. When significant degradation of the masonry units occurred, at drift levels of approximately 0.5%, a one-sided pushover test was performed. The lateral strength remained almost constant until the maximum measured drift, at which point all masonry walls experienced significant damage, with outer masonry block shells falling and vertical diaphragms inside the masonry units being crushed. Damage was concentrated in certain areas, mostly at the masonry-column interface.

To clarify the results, the masonry infill walls using solid-clay brick units developed initial cracks at drifts ranging from 0.13 to 0.17%, during which their stiffness decreased but lateral load carrying capacity increased up to drifts of about 1.5%. These cracks were distributed throughout the infill area and opened and closed under lateral load reversals without any reduction in strength. The anchors at the column–wall interface contributed to the composite behaviour of the strengthened infilled frame elements, leading to a greater number of smaller cracks accumulating in this area, particularly in specimens TYPE 1/I, TYPE 2/I, and TYPE 3/I. Additionally, relatively small cracks formed at the plastic hinge joints of the columns and beams in all specimens, with sizes under 0.4 mm for drifts under 1.0%. At larger drifts, concrete spalling appeared at the bottom of the concrete columns. The final crack patterns that developed at the maximum measured drift are presented in Figure 6.
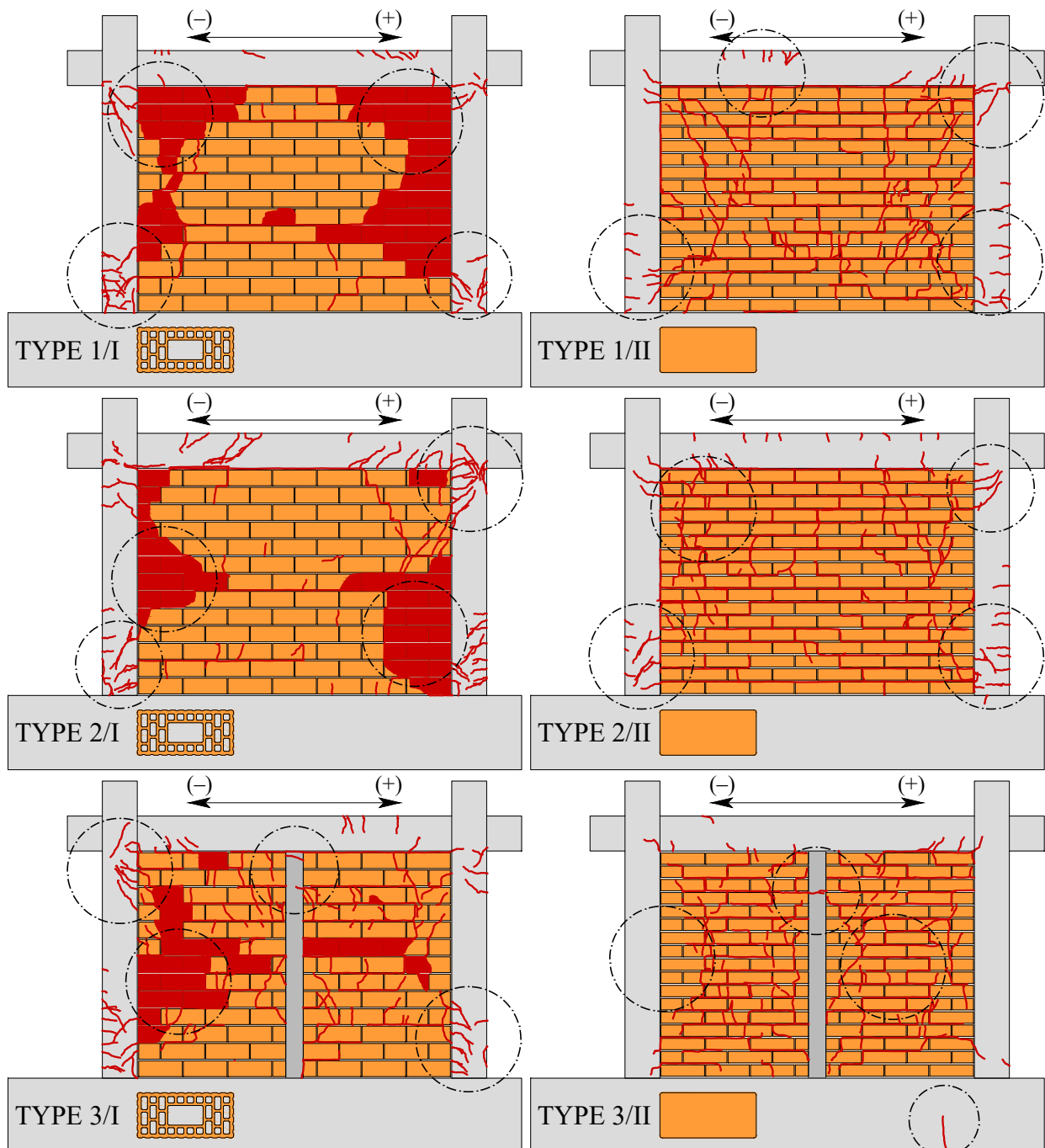
Figure 6. Crack patterns of RC beams, columns and masonry–infill of all tested specimens.

The crack patterns shown in Figure 6 correspond to the final stage of the experiment. The highest measured drift values (IDR_{MAX}) at the end of the tests were as follows: TYPE 1/I (1.14%), TYPE 2/I (1.50%), TYPE 3/I (1.50%), TYPE 1/II (1.18%), TYPE 2/II (1.21%), TYPE 3/II (1.14%).

The extent of damage was evaluated based on the severity of the damage, and damage intensity was classified into four grades (summarised in Table 2), following the EMS-98 [52] for RC systems with masonry infills. The grades range from negligible to very heavy damage (Grade 1 to Grade 4). The tests were stopped when the damage reached either Grade 4 or the maximum capacity of the test setup. Previous experiments on strengthened infilled frame structures showed that major damage occurred at the masonry infill wall, with little or no damage to the structural elements. The damage grade was assigned based on the maximum damage grade achieved by either of the composite structural elements and is graphically summarised in Figure 7.

The masonry infill walls with hollow-clay units failed in a non-ductile mode due to local brittle failure of units, resulting in buckling and crushing of thin shells and webs. The ductility and shear resistance capacity of such walls (TYPE 2/I and TYPE 3/I) were only slightly improved compared to the reference infilled frame (TYPE 1/REF). The actual resistance was only slightly greater than in the case where the walls were not strengthened at all. The referent frame specimen (TYPE 1/REF) had a higher initial stiffness but smaller drifts attributed to damage Grade 1 and Grade 2. The strengthened damaged frames had a lower initial stiffness but attained the same base shear capacity at higher drifts. All applied strengthening methods prevented strength decay within the measured drift range (<1.2%).
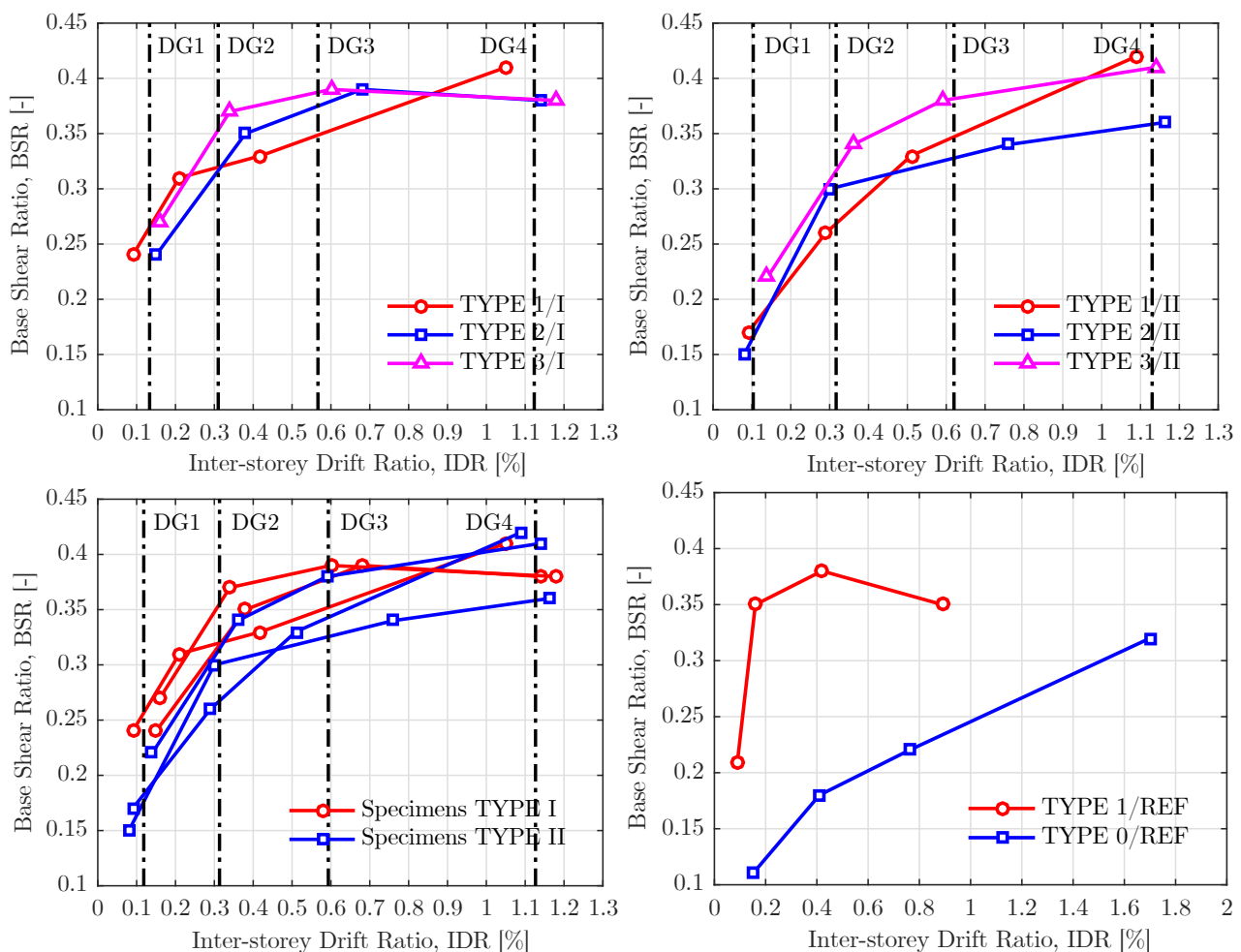

Figure 7. Trends of damage formation for all tested specimens with marked average damage limits in accordance with the EMS-98.

Table 2. Observed performance and damage grades of the tested specimens.

Specimen	Negligible to Slight Damage		Moderate Damage		Substantial to Heavy Damage		Very Heavy Damage	
	Grade 1		Grade 2		Grade 3		Grade 4	
	IDR [%]	BSR [–]	IDR [%]	BSR [–]	IDR [%]	BSR [–]	IDR [%]	BSR [–]
TYPE 1/I	0.09	0.24	0.21	0.31	0.42	0.33	1.05	0.41
TYPE 2/I	0.15	0.24	0.38	0.35	0.68	0.39	1.14	0.38
TYPE 3/I	0.16	0.27	0.34	0.37	0.60	0.39	1.18	0.38
TYPE 1/II	0.09	0.17	0.29	0.26	0.51	0.33	1.09	0.42
TYPE 2/II	0.08	0.15	0.30	0.30	0.76	0.34	1.16	0.36
TYPE 3/II	0.14	0.22	0.36	0.34	0.59	0.38	1.14	0.41
TYPE 1/REF	0.09	0.21	0.16	0.35	0.42	0.38	0.89	0.35
TYPE 0/REF	0.15	0.11	0.41	0.18	0.76	0.22	1.70	0.32

Inter-storey drift ratio (IDR) represents measured drift, i.e., represents measured displacement divided by the storey height and base shear ratio (BSR) represents measured lateral force divided by the total vertical load (the total vertical force is considered constant, as the value of 730 kN in total).

The amount of drift required to reach the same level of damage varied depending on the type of masonry unit and how it was connected to the RC frame elements. The connection between the masonry wall and the RC frame elements improved the ductility of the strengthened infilled frame structures. Solid-clay brick units prevented strength decay after reaching Damage Grade 3. Compared to the bare-frame structure, the base shear capacity of all strengthened infilled frame structures was higher at different levels of drift, with the specimens with solid-clay brick units (TYPE 1/II, 2/II, and 3/II) experiencing less damage on the RC frame elements. Most of the input energy was dissipated through horizontal shear sliding along the masonry units. Among these specimens, TYPE 3/II exhibited the best behaviour. Specifically, the base shear capacity was 3.6 times higher for a drift of 0.1%, 2.7 times higher for a drift of 0.21%, and 1.7 times higher for drifts of 0.35% and 1.0%.

5.2. Hysteresis Loops and Response Envelopes

Figure 8 shows the hysteresis loops and response envelope curves of the strengthened infilled frame models. The response envelope curves were obtained by averaging and smoothing the positive and negative branches. These curves were then used to create a bilinear idealisation and evaluate the displacement ductility, as shown in Figures 9 and 10.

The tests conducted showed that frames with masonry infill had, on average, four times greater lateral stiffness than bare frames, especially at lower drift levels, and this was not dependent on the infill type. When the masonry wall was constructed with hollow-clay masonry units, specimens with TYPE 2/I and 3/I had behaviour similar to the undamaged TYPE 1/REF specimen.

At drifts of about 0.10 to 0.15% (*Damage Grade 1*), cracking of the infill with a change of stiffness occurred. Pronounced yielding of the system occurred at drifts of about 0.20% (*Damage Grade 2*), and there was no significant stiffness change up to the ultimate drifts. The use of solid-clay brick masonry units improved the behaviour of the damaged strengthened infilled frame structures, both in capacity and ductility. At drifts of about 0.15 to 0.20% (*Damage Grade 1*), cracking of the infill occurred with a change of stiffness, and this happened at lower base shear ratios than in the case of hollow-clay units. This could be attributed to the higher initial cohesion of the mortar. After this initial change of stiffness, there was no further stiffness deterioration. Shear strength constantly increased up to the maximum measured drift, regardless of the strengthening type. The addition of the masonry infill wall within the damaged RC frames changed their behaviour, improving stiffness, base shear capacity, and damping, and making the behaviour similar to that of undamaged RC frames with masonry infill.
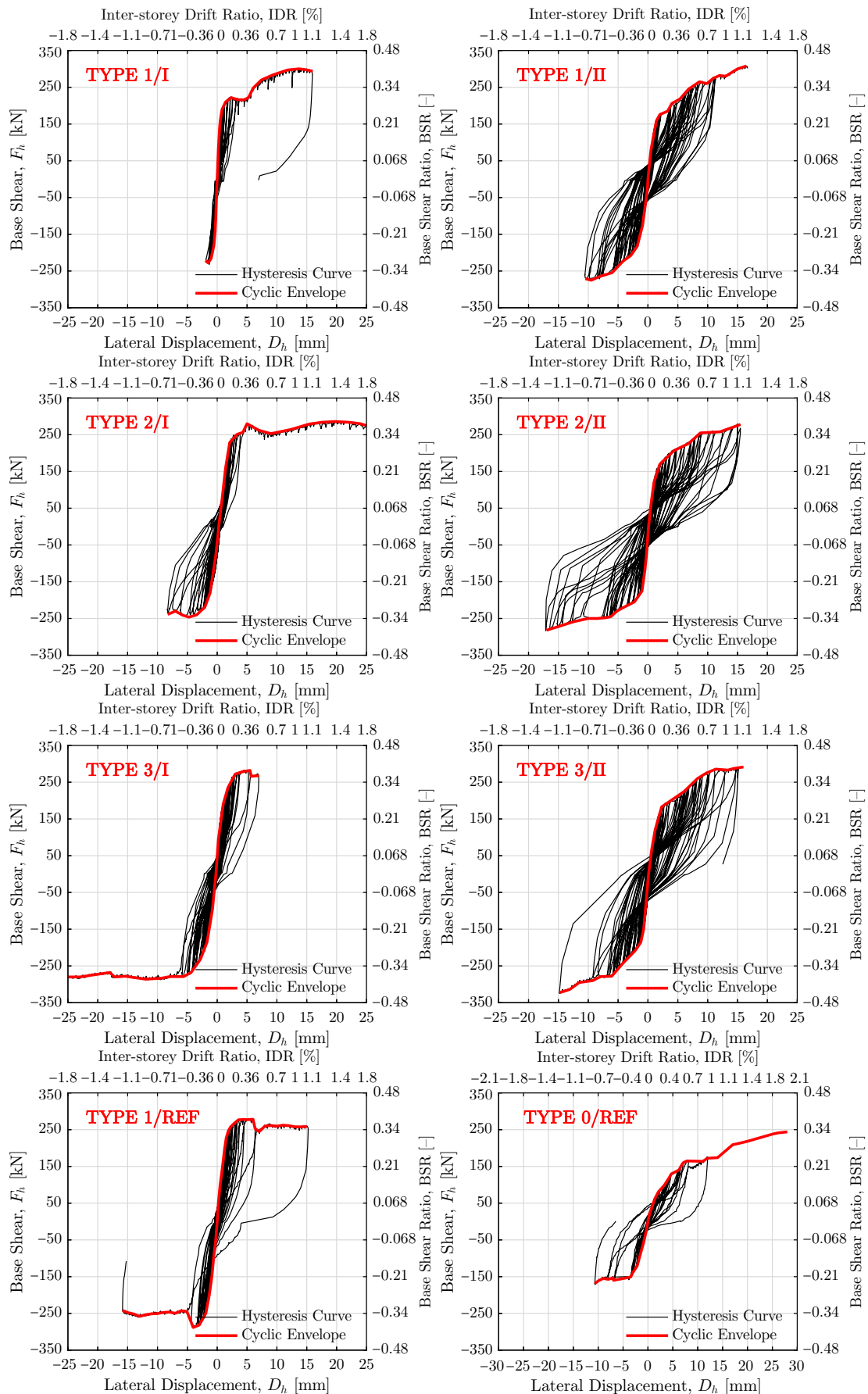
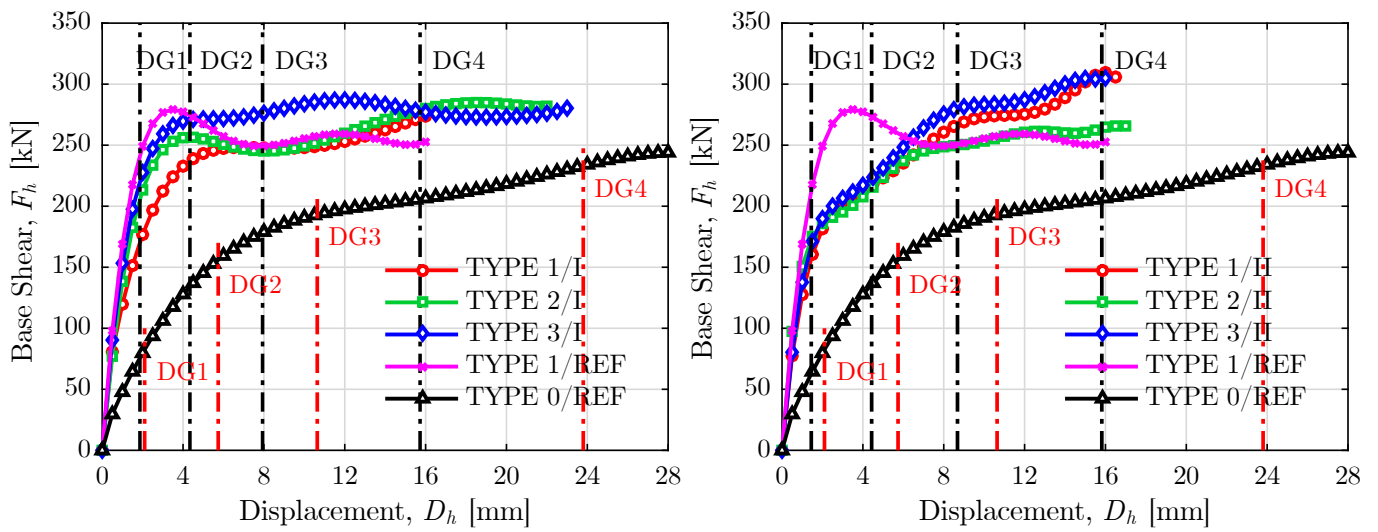**Figure 8.** Base shear—top displacement relations for all tested specimens.

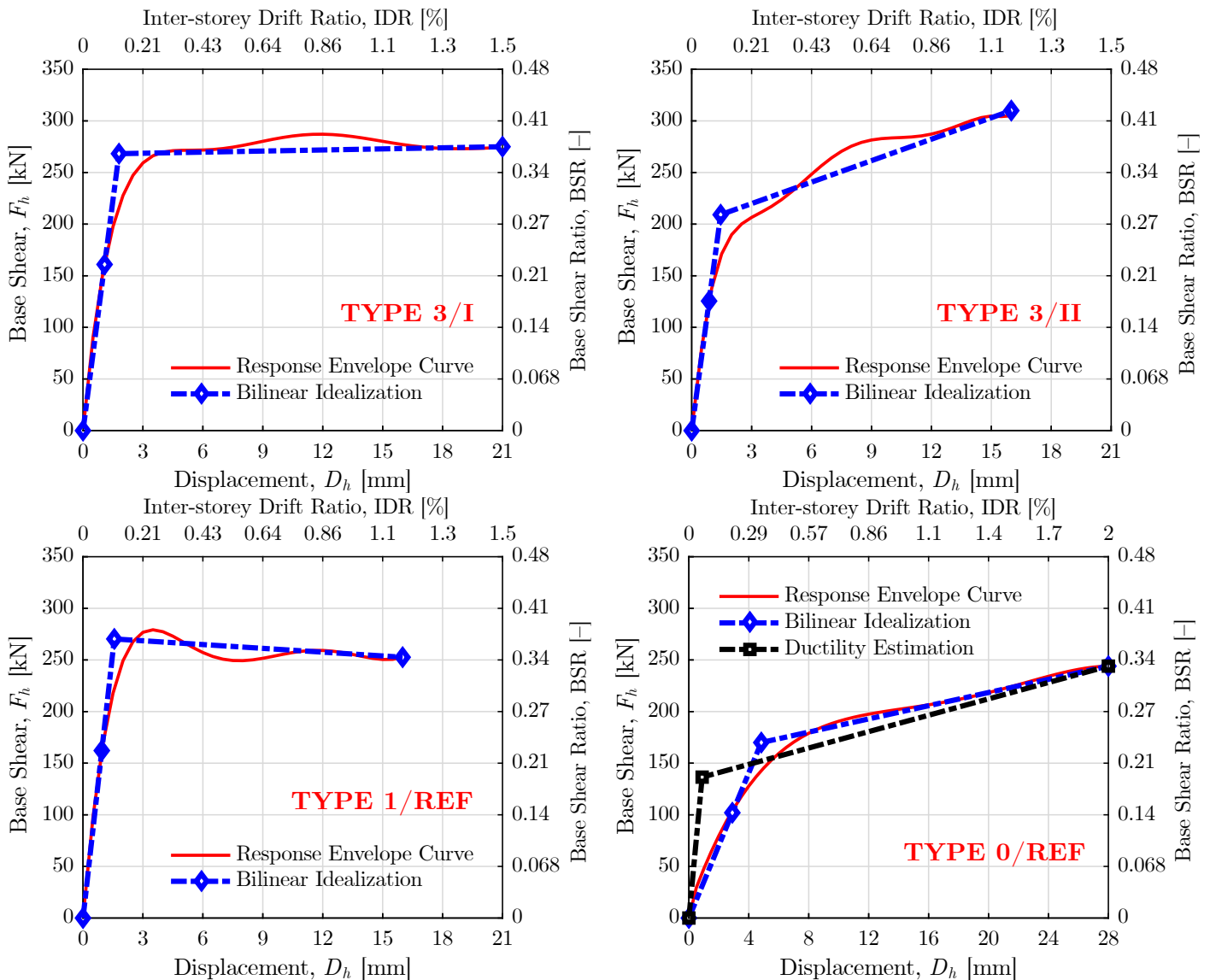**Figure 9.** Averaged response envelope curves for all tested specimens

Figure 10. Bilinear idealisation of the response envelope curves for reference and TYPE 3 specimens

Current design practices are based on the assumption that a large energy dissipation capacity is necessary to mitigate the effects induced by earthquakes. This assumption has very often led to the notion that a good structural system should be characterised by *fat* hysteresis loops. Based on the data presented in Figure 8, it can be concluded that TYPE 1/II, 2/II, and 3/II specimens produced stable hysteresis loops, indicating that solid-clay masonry units are strong and resistant to local brittle failure. When subjected to cyclic horizontal loading, solid-clay brick walls slide on their horizontal mortar joints, while walls made of blocks with vertical holes exfoliate and crush. Solid-clay brick walls exhibit wider hysteresis loops, meaning they can dissipate more energy without rapidly losing lateral bearing capacity. The detailed connections in the solid-clay brick walls increase their ductility and capacity for energy dissipation. These walls respond well beyond their elastic limit and develop a ductile inelastic response with a large dissipation capacity, even at small drifts.

The ability of the strengthened infilled frame specimens to dissipate hysteretic energy loading can be represented by the equivalent viscous damping (EVD) defined as [57]:

$$\zeta_{eq} = \frac{1}{4\pi} \cdot \frac{E_D}{E_{So}} \tag{1}$$

where E_D is energy dissipated in the specimens, i.e., the area enclosed by each hysteretic loop and E_{So} is the amount of elastic strain energy stored in the same loop (Figure 11).
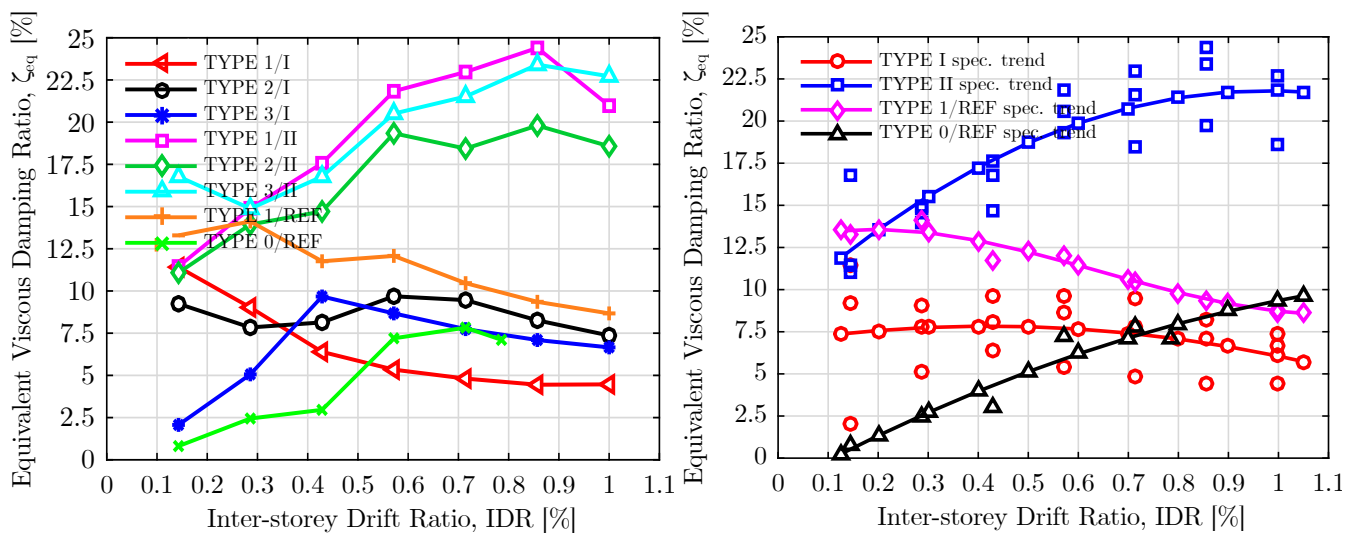

Figure 11. Equivalent viscous damping ratios (**left**) and their average trend lines (**right**).

Figure 11 shows the equivalent viscous damping ratios calculated using Equation (1) for all specimens (left) and their trend lines for different types of masonry units (right). The strengthened infilled frame specimens had higher equivalent viscous damping than the bare-frame specimen, particularly at drifts less than 1%. This is consistent with previous studies [58] and depends more on the type of masonry unit than the applied strengthening method. For drifts of about 0.4% (DG3) and 0.8% (DG4), the equivalent viscous damping was approximately 8% for hollow-clay masonry units and about 17% and 20% for solid-clay units. In comparison, the bare-frame specimen had only about 2.5% and 7.5%, respectively. The addition of the masonry infill wall in the RC frame improved the hysteretic energy-dissipation capacity by two (for hollow-clay masonry units) and by three (for solid-clay masonry units) times at drifts of 0.5%, and by two times (for solid-clay masonry units) at drifts of 1.0%.

5.3. Bilinear Idealisation of the Response Envelopes

The response envelope curves for all specimens were obtained and represented using a bilinear idealisation based on FEMA 356 [59], as shown in Figure 10 and Table 3. To calculate the effective elastic stiffness (K_{EL}) and effective yield strength (F_Y) of each specimen, a bilinear relationship was used to represent the nonlinear force-displacement relationship between base shear and displacement of the control node. The bilinear relationship was chosen because the specimens' capacity did not decline within the measured range. The base shear drift relationship was presented with an initial slope K_{EL} and post-yield slope α ($\alpha = \frac{K_{PL}}{K_{EL}}$). The effective lateral stiffness, K_{EL}, was calculated for the base shear force equal to 60% of the effective yield strength of the structure. The post-yield slope, α, was determined using an iterative graphical procedure that balanced the area above and below the curve by drawing a line segment that passed through the actual curve at the calculated target displacement.

Table 3. Characteristic points on the models' idealised bilinear curve.

Response Characteristics		TYPE 1/I	TYPE 2/I	TYPE 3/I	TYPE 1/II	TYPE 2/II	TYPE 3/II	TYPE 0/REF	TYPE 1/REF
F_Y	[kN]	215	246	268	200	210	209	170	270
F_{MAX}	[kN]	274	282	275	306	266	310	244	253
D_Y	[mm]	1.9	1.8	1.8	1.8	1.7	1.6	4.8	1.6
D_{MAX}	[mm]	16.0	21.0	21.0	16.5	17.0	16.0	28.0	16.0
IDR_{MAX}	[%]	1.14	1.50	1.50	1.18	1.21	1.14	2.00	1.14
K_{EL}	[kN/mm]	113.2	136.7	148.9	111.1	123.5	130.6	35.2	172.6
K_{PL}	[kN/mm]	4.2	1.9	0.4	7.2	3.7	7.0	3.2	−1.2
α	[−]	0.037	0.014	0.003	0.065	0.030	0.054	0.091	−0.007

F_Y is yield strength, F_{MAX} is maximum achieved strength, D_Y is yield displacement, D_{MAX} is displacement at maximum achieved strength, IDR_{MAX} is drift at maximum achieved strength [%], K_{EL} is initial/elastic stiffness, K_{PL} is post–yield/plastic stiffness, α is post–yield slope, $\alpha = \frac{K_{PL}}{K_{EL}}$.

The behaviour of the system is evaluated using bilinear idealisation, and the results are shown in Table 4. It is observed that the undamaged and strengthened infilled frame structures have similar base shear and drift capacity, as well as behaviour factors. For the bare-frame and strengthened infilled frame specimens, two bilinear idealisations are presented for specimen TYPE 0/REF. One is obtained similarly to the other frames, and the other has an initial stiffness taken as the average of the initial stiffness of all other specimens. The behaviour factor, $q*$, for the investigated wall groups, is calculated using an approximation of Equation (2) as suggested in [60,61] and described in detail in [61].

This equation neglects the soil-structure interaction and equalises the linear and nonlinear system energy:

$$q* = \sqrt{(2 \cdot \mu_U - 1)} \tag{2}$$

where μ_U refers to the ductility ratio which is defined as $\mu_U = \frac{D_{MAX}}{D_Y}$ whose values are shown in Table 4. The calculated behaviour factors indicate that all strengthened infilled frame specimens had behaviour factors more than two times those suggested for confined masonry walls ($q = 2.0$ to 3.0) [49]. Based on the results obtained in this and similar experiments, the behaviour factor to be used in the linear analysis may be redefined through the introduction of the over-strength ratio (OSR) $\frac{F_U}{F_{EL}}$, where F_U stands for the ultimate horizontal bearing capacity, while F_{EL} stands for the base shear value corresponding to the first failure, i.e., elastic capacity [61,62].

Here, the over-strength ratio (OSR) brought an increase of more than 30% (for solid-clay masonry units) of the basic behaviour factor, indicating the possibility of reducing the design forces for linear elastic analysis with respect to the values traditionally used in the seismic codes for the design of the buildings of this type.

Table 4. Measured ultimate base shear capacity, drifts, ductility, over-strength ratios, and behaviour factors.

Specimens	F_{MAX} [kN] Ultimate Load Capacity	IDR_{MAX} [%] Max. Inter-Storey Drift Ratio	$\mu_U = \frac{D_{MAX}}{D_Y}$ Ductility Ratio	OSR Over-Strength Ratio	$q* = \sqrt{(2 \cdot \mu_U - 1) \cdot OSR}$ Behaviour Factor/Behaviour Factor·OSR
TYPE 1/I	274	1.14	8.35	1.27	3.96/5.04
TYPE 2/I	282	1.50	11.46	1.15	4.68/5.36
TYPE 3/I	275	1.50	11.67	1.03	4.73/4.83
TYPE 1/II	306	1.18	11.00	1.54	4.58/7.04
TYPE 2/II	266	1.21	14.17	1.27	5.23/6.62
TYPE 3/II	310	1.14	11.03	1.48	4.59/6.80
TYPE 1/REF	253	1.14	10.21	0.93	4.41/4.12
TYPE 0/REF	244	2.00	5.79 (31.64)	1.44 (1.79)	3.25 (7.89)/4.67 (14.11)

6. Conclusions and Remarks

In many instances, masonry infill walls offer benefits as they function like a weaker version of the shear wall. Given the favourable impacts of infills and their cost-effective construction, authors have suggested using them as strengthening elements within the existing RC frame buildings. This research's main objective and novelty involve investigating the advantages of incorporating different traditional reinforced masonry infills into existing RC frames to improve seismic resistance, mostly in terms of improved stiffness, lateral load capacity, and better energy dissipation ability.

As such, this study analyses six ductile and insignificantly damaged RC frames that have been strengthened using three strengthening techniques and two types of masonry units (hollow-clay and solid-clay units), alongside two reference specimens. The RC frame specimens were damaged during two previous tests, where they underwent drifts larger than 1.5%. They were repaired by replacement of the spalled and cracked concrete. Strengthened infilled frame structures were tested under constant vertical and cyclic lateral loading.

It was observed that damaged RC frames strengthened by the addition of the masonry infill walls had behaviour similar to that of the undamaged infilled RC frames. Strengthened infilled frame structures had increased stiffness, strength, and hysteretic damping. The stiffness increased irrespective of the masonry units and applied strengthening method. Strength and hysteretic damping depended on the masonry units, especially their robustness, and applied method. Hollow-clay masonry units degraded due to their small robustness and interlocking of the mortar and clay shells. Their contribution to the strength and hysteretic damping was negligible after drifts of 0.5% and behaved in a fragile manner. Solid-clay masonry units proved better and strengthened infilled frame elements had no strength and hysteretic energy damping decay, even after drifts of 1.2%.

Hysteretic energy-dissipation capacity depended on the masonry units' robustness and was much better for solid-clay than hollow-clay units. The equivalent viscous damping ratio increased by two (for hollow-clay masonry units) to three (for solid-clay masonry units) times at drifts of 0.5%, and by two times (for solid-clay masonry units) at drifts of 1%. There was no significant difference in the observed response among various types of connection between infill and frame. The best option proved the addition of the masonry wall strengthened with additional vertical tie-column and connected to it and the surrounding frame by steel dowels. The presence of the tie-column increased in-plane ductility and may have a beneficial effect on out-of-plane stability and resilience, which are not part of this study.

The calculated behaviour factor of the strengthened infilled frame structures was between the values suggested for confined-masonry and RC frame structures. The over-strength ratio (OSR) brought an increase of more than 30% to the behaviour factor in the case of solid-clay masonry units. Therefore, strengthened infilled frame structures could only unfavourably be calculated as confined-masonry structures. The strength-

ened structures sustained drift reversals with amplitudes of up to 1.2% without excessive strength reduction.

Since the experimental tests did not bring the test specimens to the collapse limit, future research must investigate the benefits of such strengthening on the ultimate limit states of collapse, particularly for seismic risk analysis and loss assessment of such RC buildings. Moreover, for future research, different types of anchoring for different diameters of reinforcing bars of reinforced masonry infill should be thoroughly examined, at least numerically. Because these variations can result in various failure mechanisms, it is necessary to parametrically analyse the optimal combination of infill reinforcement, infill-frame connection, and mechanical properties of masonry infill (masonry element and mortar).

Abbreviations

The following abbreviations are used in this manuscript (in alphabetical order):

BCC	Beam-column joint crack
BSR	Base Shear Ratio
CC	Corner Crushing
COV	Coefficients Of Variation
DC	Diagonal Compression
DCM	Ductility Class Medium
DG	Damage Grade
EC2	Eurocode 2
EC8	Eurocode 8
ECC	Engineered Cementitious Composites
EMS	European Macroseismic Scale
EVD	Equivalent Viscous Damping
FEMA	Federal Emergency Management Agency
FRP	Fibre Reinforced Polymer
HSS	Horizontal Sliding Shear
IDR	Inter-storey Drift Ratio
LVDT	Linear Variable Differential Transformer
MRF	Moment Resisting Frames
NSM	Near Surface Mounted
OSR	Over-Strength Ratio
PCP	Precast Concrete Panels
RC	Reinforced Concrete
SC	Shear cracking failure of the columns
SS	Bed Joint Sliding Shear
TC	Tensile cracking failure of the columns
TLD	Tuned Liquid Damper
TMD	Tuned Mass Damper
TRM	Textile Reinforced Mortar

References

1. Gkournelos, P.; Triantafillou, T.; Bournas, D. Seismic upgrading of existing reinforced concrete buildings: A state-of-the-art review. *Eng. Struct.* **2021**, *240*, 112273. [CrossRef]
2. Anand, P.; Sinha, A.K. Seismic Strengthening and Retrofitting Techniques and Solutions for an Existing RC Frame: An Overview. In *A System Engineering Approach to Disaster Resilience*; Ghosh, C., Kolathayar, S., Eds.; Springer Nature: Singapore, 2022; pp. 531–539.
3. Valente, M.; Milani, G. Alternative retrofitting strategies to prevent the failure of an under-designed reinforced concrete frame. *Eng. Fail. Anal.* **2018**, *89*, 271–285. [CrossRef]
4. Pujol, S.; Fick, D. The Test of a Full–scale Three–story RC Structure with Masonry Infill Walls. *Eng. Struct.* 2010, *32*, 3112–3121. [CrossRef]
5. Kalman Šipoš, T.; Sigmund, V.; Hadzima-Nyarko, M. Earthquake Performance of Infilled Frames Using Neural Networks and Experimental Database. *Eng. Struct.* **2013**, *51*, 113–127. [CrossRef]
6. Kalman Šipoš, T.; Rodrigues, H.; Grubišić, M. Simple design of masonry infilled reinforced concrete frames for earthquake resistance. *Eng. Struct.* **2018**, *171*, 961–981. [CrossRef]
7. Furtado, A.; Rodrigues, H.; Arêde, A. Cantilever flexural strength tests of masonry infill walls strengthened with textile-reinforced mortar. *J. Build. Eng.* **2021**, *33*, 101611. [CrossRef]
8. Martinelli, E.; Lima, C.; Stefano, G.D. A simplified procedure for Nonlinear Static analysis of masonry infilled RC frames. *Eng. Struct.* **2015**, *101*, 591–608. [CrossRef]
9. Sigmund, V.; Penava, D. Influence of Openings, With and Without Confinement, on Cyclic Response of Infilled RC Frames—An Experimental Study. *J. Earthq. Eng.* **2014**, *18*, 113–146.
10. Grubišić, M. Models for Strengthening Assessment of Reinforced Concrete Frames by Adding the Infills for Earthquake Action. Ph.D. Thesis, Faculty of Civil Engineering Osijek, University of Osijek, Osijek, Croatia, 2016. Available online: https://repozitorij.gfos.hr/islandora/object/gfos:883 (accessed on 12 March 2023).
11. Blasi, G.; Luca, F.D.; Aiello, M.A. Brittle failure in RC masonry infilled frames: The role of infill overstrength. *Eng. Struct.* **2018**, *177*, 506–518. [CrossRef]
12. Risi, M.T.D.; Gaudio, C.D.; Ricci, P.; Verderame, G.M. In-plane behaviour and damage assessment of masonry infills with hollow clay bricks in RC frames. *Eng. Struct.* **2018**, *168*, 257–275. [CrossRef]
13. Furtado, A.; Rodrigues, H.; Arêde, A.; Varum, H. Experimental tests on strengthening strategies for masonry infill walls: A literature review. *Constr. Build. Mater.* **2020**, *263*, 120520. [CrossRef]
14. Palieraki, V.; Zeris, C.; Vintzileou, E.; Adami, C.E. In-plane and out-of plane response of currently constructed masonry infills. *Eng. Struct.* **2018**, *177*, 103–116. [CrossRef]
15. Usta, P.; Özge Onat.; Özgür Bozdağ. Effect of masonry infill walls on the nonlinear response of reinforced concrete structure: October 30, 2020 İzmir earthquake case. *Eng. Fail. Anal.* **2023**, *146*, 107081. [CrossRef]
16. Maidiawati.; Tanjung, J.; Nazri, F.M.; Hayati, Y.; Masrilayanti. A Simple Strengthening Method for Preventing Collapsed of Vulnerable Masonry Infills. *Buildings* **2022**, *12*, 1496. [CrossRef]
17. Altin, S.; Özgür Anil.; Kara, M.E.; Kaya, M. An experimental study on strengthening of masonry infilled RC frames using diagonal CFRP strips. *Compos. Part B Eng.* **2008**, *39*, 680–693. [CrossRef]
18. Koutas, L.; Pitytzogia, A.; Triantafillou, T.C.; Bousias, S.N. Strengthening of Infilled Reinforced Concrete Frames with TRM: Study on the Development and Testing of Textile-Based Anchors. *J. Compos. Constr.* **2014**, *18*, A4013015. [CrossRef]
19. Koutas, L.; Triantafillou, T.C.; Bousias, S.N. Analytical Modeling of Masonry-Infilled RC Frames Retrofitted with Textile-Reinforced Mortar. *J. Compos. Constr.* **2015**, *19*, 04014082. [CrossRef]
20. Koutas, L.; Bousias, S.N.; Triantafillou, T.C. Seismic Strengthening of Masonry-Infilled RC Frames with TRM: Experimental Study. *J. Compos. Constr.* **2015**, *19*, 4014048. [CrossRef]
21. Fiorato, A.E.; Sozen, M.A.; Gamble, W.L. *An Investigation of the Interaction of Reinforced Concrete Frames with Masonry Filler Walls*; Technical Report; University of Illinois Engineering Experiment Station, College of Engineering, University of Illinois at Urbana–Champaign: Champaign, IL, USA, 1970.
22. Brokken, S.T.; Bertero, V.V. Studies on Effects of Infills in Seismic Resistant RC Construction. *NASA STI/Recon Tech. Rep. N* **1981**, *82*, 31576.
23. Calvi, G.M.; Bolognini, D. Seismic Response of Reinforced Concrete Frames Infilled with Weakly Reinforced Masonry Panels. *J. Earthq. Eng.* **2001**, *5*, 153–185.
24. Negro, P.; Verzeletti, G. Effect of Infills on the Global Behaviour Of RC Frames: Energy Considerations from Pseudodynamic Tests. *Earthq. Eng. Struct. Dyn.* **1996**, *25*, 753–773. [CrossRef]
25. Žarnić, R.; Gostič, S.; Crewe, A.J.; Taylor, C.A. Shaking Table Tests of 1:4 Reduced–scale Models of Masonry Infilled Reinforced Concrete Frame Buildings. *Earthq. Eng. Struct. Dyn.* **2001**, *30*, 819–834. [CrossRef]
26. Hashemi, A.; Mosalam, K.M. Shake–table Experiment on Reinforced Concrete Structure Containing Masonry Infill Wall. *Earthq. Eng. Struct. Dyn.* **2006**, *35*, 1827–1852. [CrossRef]
27. Ricci, P.; Domenico, M.D.; Verderame, G.M. Experimental assessment of the in–plane/out–of–plane interaction in unreinforced masonry infill walls. *Eng. Struct.* **2018**, *173*, 960–978. [CrossRef]

28. Morandi, P.; Hak, S.; Magenes, G. Mechanical characterization and force–displacement hysteretic curves from in–plane cyclic tests on strong masonry infills. *Data Brief* **2018**, *16*, 886–904. [CrossRef]

29. Roosta, S.; Liu, Y. Behavior of concrete masonry infills bounded by masonry frames subjected to in-plane lateral loading—Experimental study. *Eng. Struct.* **2021**, *247*, 113153. [CrossRef]

30. Trapani, F.D.; Bolis, V.; Basone, F.; Preti, M. Seismic reliability and loss assessment of RC frame structures with traditional and innovative masonry infills. *Eng. Struct.* **2020**, *208*, 110306. [CrossRef]

31. Baniahmadi, M.; Vafaei, M.; Alih, S.C. Cyclic response of reinforced concrete frames partially infilled with relatively weak masonry wall. *J. Build. Eng.* **2022**, *46*, 103722. [CrossRef]

32. Dehghani, A.; Nateghi-Alahi, F.; Fischer, G. Engineered cementitious composites for strengthening masonry infilled reinforced concrete frames. *Eng. Struct.* **2015**, *105*, 197–208. [CrossRef]

33. Furtado, A.; Rodrigues, H.; Arede, A.; Varum, H.; Grubišić, M.; Šipoš, T. Prediction of the earthquake response of a three–storey infilled RC structure. *Eng. Struct.* **2018**, *171*, 214–235. [CrossRef]

34. Shimazaki, K. Strong Ground Motion Drift and Base Shear Coefficient for RC Structures. In Proceedings of the Ninth World Conference on Earthquake Engineering, Tokyo-Kyoto, Japan, 2–9 August 1988; Volume V.

35. Wood, S.L. Performance of Reinforced Concrete Buildings During the 1985 Chile Earthquake: Implications for the Design of Structural Walls. *Earthq. Spectra* **1991**, *7*, 607–638. [CrossRef]

36. Lepage, A. A Method for Drift–Control in Earthquake–Resistant Design of RC Building Structures. Ph.D. Thesis, University of Illinois, Urbana, Urbana, IL, USA, 1997.

37. Marinković, M.; Butenweg, C. Experimental testing of decoupled masonry infills with steel anchors for out-of-plane support under combined in-plane and out-of-plane seismic loading. *Constr. Build. Mater.* **2022**, *318*, 126041. [CrossRef]

38. Leeanansaksiri, A.; Panyakapo, P.; Ruangrassamee, A. Seismic capacity of masonry infilled RC frame strengthening with expanded metal ferrocement. *Eng. Struct.* **2018**, *159*, 110–127. [CrossRef]

39. Noh, N.M.; Liberatore, L.; Mollaioli, F.; Tesfamariam, S. Modelling of masonry infilled RC frames subjected to cyclic loads: State of the art review and modelling with OpenSees. *Eng. Struct.* **2017**, *150*, 599–621. [CrossRef]

40. Morandi, P.; Milanesi, R.R.; Magenes, G. Innovative solution for seismic-resistant masonry infills with sliding joints: In-plane experimental performance. *Eng. Struct.* **2018**, *176*, 719–733. [CrossRef]

41. Morfidis, K.; Kostinakis, K. The role of masonry infills on the damage response of R/C buildings subjected to seismic sequences. *Eng. Struct.* **2017**, *131*, 459–476. [CrossRef]

42. *HRN EN 1998-1:2011/NA:2011*; Eurokod 8: Projektiranje Potresne Otpornosti Konstrukcija—1.dio: Opća Pravila, Potresna Djelovanja i Pravila za Zgrade—Nacionalni Dodatak. Croatian Standards Instutute/Hrvatski zavod za Norme (HZN): Zagreb, Croatia, 2011.

43. Miranda, E.; Brzev, S.; Bijelic, N.; Arbanas, Ž.; Bartolac, M.; Jagodnik, V.; Lazarević, D.; Mihalić Arbanas, S.; Zlatović, S.; Acosta Vera, A.; et al. *StEER-EERI: Petrinja, Croatia December 29, 2020, Mw 6.4 Earthquake Joint Reconnaissance Report (JRR)*; Technical Report; EERI: Zagreb, Croatia, 2020.

44. Cao, X.Y.; Feng, D.C.; Beer, M. Consistent seismic hazard and fragility analysis considering combined capacity-demand uncertainties via probability density evolution method. *Struct. Saf.* **2023**, *103*, 102330. [CrossRef]

45. Cao, X.Y.; Shen, D.; Feng, D.C.; Wang, C.L.; Qu, Z.; Wu, G. Seismic retrofitting of existing frame buildings through externally attached sub-structures: State of the art review and future perspectives. *J. Build. Eng.* **2022**, *57*, 104904. [CrossRef]

46. Almusallam, T.H.; Al-Salloum, Y.A. Behavior of FRP Strengthened Infill Walls under In-Plane Seismic Loading. *J. Compos. Constr.* **2007**, *11*, 308–318. [CrossRef]

47. Sigmund, V. *Seismic Design of Infilled Frames*; Technical Report, Research Project No. 149–1492966–1536; Faculty of Civil Engineering, Josip Juraj Strossmayer University of Osijek: Osijek, Croatia, 2007–2013.

48. *EN 1992-1:2004*; Eurocode 2—Design of Concrete Structures—Part 1: General Rules and Rules for Buildings. European Committee for Standardization, CEN: Brussels, Belgium, 2004.

49. *EN 1998-1:2004*; Eurocode 8—Design of Structures for Earthquake Resistance—Part 1: General Rules, Seismic Actions and Rules for Buildings. European Committee for Standardization, CEN: Brussels, Belgium, 2004.

50. *EN 1998-3:2005*; Eurocode 8—Design of Structures for Earthquake Resistance—Part 3: Assessment and Retrofitting of Buildings. European Committee for Standardization, CEN: Brussels, Belgium, 2005.

51. Zovkić, J.; Sigmund, V.; Guljaš, I. Cyclic Testing of a Single Bay Reinforced Concrete Frames With Various Types of Masonry Infill. *Earthq. Eng. Struct. Dyn.* **2013**, *42*, 1131–1149. [CrossRef]

52. Grünthal, G. *European Macroseismic Scale 1998—EMS–98*; Technical Report; Cahiers du Centre Européen de Geodynamique et de Seismologie: Luxembourg, 1998; Volume 15.

53. Penava, D.; Radić, I.; Gazić, G.; Sigmund, V. Mechanical Properties of Masonry as Required for the Seismic Resistance Verification. *Tech. Gaz.* **2011**, *18*, 273–280.

54. Matošević, D.; Sigmund, V.; Guljaš, I. Cyclic testing of single bay confined masonry walls with various connection details. *Bull. Earthq. Eng.* **2015**, *13*, 565–586. [CrossRef]

55. Kabeyasawa, T.; Shiohara, H.; Otani, S.; Aoyama, H. Analysis of The Full-Scale Seven-Story Reinforced Concrete Test Structure. *J. Fac. Eng. Univ. Tokyo* **1983**, *37*, 431–478. [CrossRef]

56. Murty, C.V.R.; Jain, S.K. Beneficial Influence of Masonry Infill Walls on Seismic Performance of RC Frame Buildings. In Proceedings of the 12th World Conference on Earthquake Engineering (12WCEE), Auckland, New Zealand, 30 January–4 February 2000; p. 1790.

57. Shibata, A.; Sozen, M.A. Substitute–Structure Method for Seismic Design in R/C. *J. Struct. Div.* **1976**, *102*, 1–18. [CrossRef]

58. Landi, L.; Diotallevi, P.P.; Tardini, A. Equivalent Viscous Damping for the Displacement–Based Seismic Assessment of Infilled RC Frames. In Proceedings of the 15th World Conference on Earthquake Engineering (15WCEE), Lisbon, Portugal, 24–28 September 2012.

59. FEMA356. *Prestandard and Commentary for the Seismic Rehabilitation of Buildings*; Federal Emergency Management Agency, FEMA: Washington, DC, USA , 2000.

60. Tomaževič, M.; Weiss, P. Displacement Capacity of Masonry Buildings as a Basis for the Assessment of Behavior Factor: An Experimental Study. *Bull. Earthq. Eng.* **2010**, *8*, 1267–1294. [CrossRef]

61. Frumento, S.; Magenes, G.; Morandi, P.; Calvi, G.M. *Interpretation of Experimental Shear Tests on Clay Brick Masonry Walls and Evaluation of q-Factors for Seismic Design*; IUSS Press: Pavia, Italy, 2009. [CrossRef]

62. Morandi, P. New Proposals for Simplified Seismic Design of Masonry Buildings. Ph.D. Thesis, Rose School, Universitá degli Studi di Pavia, Pavia, Italy, 2006. [CrossRef]